

Polaris: Multi-Fidelity Design Space Exploration of Deep Learning Accelerators

Chirag Sakhuja
The University of Texas at Austin
Austin, TX, USA
chirag.sakhuja@utexas.edu

Charles Hong
University of California, Berkeley
Berkeley, CA, USA
charleshong@berkeley.edu

Calvin Lin
The University of Texas at Austin
Austin, TX, USA
lin@cs.utexas.edu

Abstract—This paper presents a tool for automatically exploring the design space of deep learning accelerators (DLAs).

Our main advancement is Starlight, a data-driven performance model that uses transfer learning to bridge the gap between fast, low-fidelity evaluation methods (such as analytical models) and slow, high-fidelity evaluation methods (such as RTL simulation). Starlight is fast: It can provide 6,500 predictions per second, allowing the evaluation of millions of configurations per hour. Starlight is accurate: It predicts the energy-delay product measured by RTL simulation with 99% accuracy. And Starlight can be trained efficiently: It can be trained with 61% fewer samples than DOSA’s state-of-the-art data-driven performance predictor [22].

Our second contribution is Polaris, a design-space exploration tool that uses Starlight to efficiently search the large, complex hardware/software co-design space of DLAs. In under 35 minutes, Polaris produces DLA designs that match the performance of designs that take six hours to produce with DOSA. And in under 3.3 hours, Polaris produces DLA designs that reduce energy-delay product by $2.7\times$ over the best designs found by DOSA.

Index Terms—AI Accelerators, Design Automation, Gaussian Processes, Transfer Learning

I. INTRODUCTION

Because of the far-reaching impact of deep learning [11], [41], modern hardware systems often incorporate deep learning accelerators (DLAs) [1], [12], [24], [37], [56], [58], [62], which for deep learning workloads are more energy- and area-efficient than CPUs and GPUs [10]. Because of the fast pace of innovation in deep learning models [7], [24], [56], new DLAs are constantly being developed.

One method of reducing the high cost [25], [36] of DLA design is to perform automated design space exploration (DSE) of the hardware/software (HW/SW) co-design space [8], [22], [23], [26], [34], [40], [43], [45], [52], [53], [63], [67]–[70]. This design space consists of design parameters, such as spatial array dimensions, memory sizes, and loop tiling factors. DSE iteratively identifies points in the design space and evaluates their quality based on some optimization criteria (e.g., minimized delay or energy-delay product).

For DSE tools, the choice of evaluation mechanism presents a fundamental tradeoff. The tool could evaluate configurations

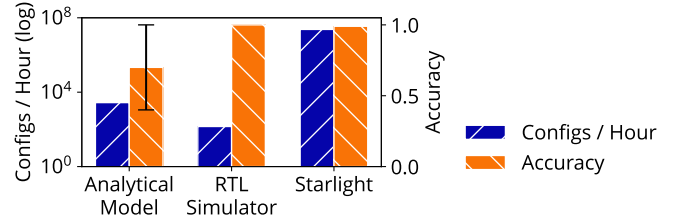


Fig. 1: Analytical models can be queried thousands of times an hour, but they are inaccurate, whereas an RTL simulator is accurate but slow. Our learned model, Starlight, breaks this tradeoff by predicting performance faster than an analytical model and with 99% accuracy when compared to an RTL simulator. These data are collected by Parashar et al. [46], Karandikar et al. [27], and Muñoz-Martinez et al. [44].

with high fidelity, e.g., using an RTL simulator, but the long latency of such techniques would restrict the DSE tool to considering just a small number of configurations, severely limiting the tool’s effectiveness. Alternatively, the tool could evaluate a large number of configurations using a fast evaluation method, e.g., an analytical model, but such techniques have low fidelity because they do not capture the nuances of circuitry or runtime behavior. Figure 1 illustrates this tradeoff: As model fidelity increases, the number of configurations that a DSE tool can evaluate dramatically decreases.

Prior work [22], [34] attempts to break this tradeoff by using a fast *data-driven model* that has been trained to predict a design’s performance as measured by a high-fidelity method, such as RTL simulation. Such a data-driven model can be queried even faster than an analytical model and can produce results that approach the accuracy of RTL simulation. Unfortunately, the training required to produce such a data-driven model itself requires thousands of high-fidelity evaluations [22], [34]—which even as a one-time investment is difficult to collect—presenting the same tradeoff that the data-driven model was intended to break.

In this paper, we break this tradeoff by employing a technique called *transfer learning* to more efficiently train a data-driven model. Transfer learning uses as a starting point an existing data-driven model that is trained on a similar but different prediction task. We use transfer learning to train a

This work was funded by a gift from ARM and by an NXP fellowship. We thank Kevin Swersky for his collaboration on foundational concepts that this paper builds on, and we thank Minesh Patel, Molly O’Neil, and Quang Duong for their comments on early drafts of this paper.

data-driven model that predicts the performance of a DLA as measured by RTL simulation; our model is trained primarily on easy-to-collect, low-fidelity evaluations (analytical model) rather than hard-to-collect, high-fidelity evaluations (RTL simulation). We are the first to apply transfer learning this way.

Figure 1 shows that our data-driven model, called Starlight, can be queried faster than an analytical model and can achieve 99% accuracy when predicting the energy-delay product (EDP) of a DLA. Moreover, Starlight is trained with 61% fewer high-fidelity evaluations and achieves higher accuracy than DOSA’s state-of-the-art data-driven model [22].

Because Starlight achieves such high accuracy, we might be tempted to perform DSE with Starlight using the *offline* approach that prior work has taken [34], namely, perform optimization (e.g., stochastic gradient descent) on Starlight and evaluate the final resulting design with RTL simulation. But even a highly accurate model may not capture details of the actual hardware, so a design that is deemed high-quality by the model might not be high-quality when translated to real hardware. Thus, it might be necessary to perform RTL simulation *in* the optimization loop, which is known as *online* DSE. Others have suggested that offline approaches are sufficient [34], but in this paper, we show for the first time that there *is* significant advantage to building an online DSE tool to ensure that the designs are faithful when translated to real hardware.

We do so by building Polaris, a DSE tool that integrates Starlight into a Bayesian optimization (BO) framework. BO is sample-efficient because it carefully selects the designs that should be evaluated using RTL simulation. In particular, Polaris uses Starlight to balance the exploitation of promising regions of the co-design space with the exploration of uncertain regions of the co-design space. Because Polaris utilizes a mixture of low- and high-fidelity evaluations, we say that it performs multi-fidelity design space exploration.

This paper makes the following contributions:

- We demonstrate that transfer learning is an effective method of building data-driven performance models. Our model is trained with 61% fewer evaluations than DOSA’s state-of-the-art data-driven model [22].
- We present Starlight, a data-driven model that predicts with 99% accuracy the EDP of a DLA as measured by RTL simulation. Transfer learning allows Starlight to be trained in 2 minutes on a consumer-grade CPU.
- We demonstrate the benefit of performing RTL simulation in the optimization loop by presenting Polaris, a DSE tool that integrates Starlight into a Bayesian optimization framework to perform hardware/software co-design of DLAs. Polaris produces in 35 minutes DLA designs and software mappings that have lower EDP than those produced in 6 hours by DOSA [22], which uses an offline approach. And within 3.3 hours, Polaris’ designs achieve an average reduction of $2.7\times$ in EDP over the best designs produced by DOSA.

The remainder of this paper is organized as follows. Section II places this work in the context of prior work. Section III

then provides background for understanding our solution. Section IV and Section V describe in greater detail Starlight and Polaris, respectively. Sections VI and VII present the evaluation methodology and evaluation results of Starlight and Polaris, and Section VIII provides concluding remarks.

II. RELATED WORK

This section places our work in the context of prior work.

A. Performance Predictors

Data-driven models are a valuable tool because they can predict the performance of a DLA with accuracy that approaches RTL simulation, but they can be queried orders of magnitude more quickly than RTL simulation.

Kaufman et al. [28] design the first general-purpose data-driven model, which is a graph neural network that estimates delay by consuming as input a tensor computation graph and DLA-specific opcodes. Esmaeilzadeh et al. [14] and Ferienc et al. [15] present data-driven models that take as input abstracted convolutional layer shapes and/or DLA architectural parameters, but they only support a subset of the design space that Starlight supports. AIRchitect [53] is a recommendation model that automatically predicts for a given workload optimized design parameters, but AIRchitect does not account for the DLA’s architectural parameters. Other data-driven models are integrated into DSE tools [13], [22], [23], [34].

Some data-driven models [14], [22], [34] are trained with samples from a slow high-fidelity method, such as RTL simulation, which are difficult to collect. Starlight is the first data-driven model to reduce the cost of training by transferring knowledge from a low-fidelity data-driven performance model to a high-fidelity data-driven performance model.

B. Automated HW/SW Co-Design of DLAs

Recent work in the automated DSE of deep learning accelerators (DLAs) [29], [47], [55], [61] commonly targets the exploration of the joint design space of architectural parameters—e.g. systolic array size—and software mappings—e.g. loop tiling factors—because the two design spaces are tightly coupled and are profitable to explore simultaneously [46], [57]. This type of DSE is called HW/SW co-design.

For modest co-design spaces, simple black-box optimization algorithms [8], [43] that require no knowledge of the shape of the objective function are feasible, but larger co-design spaces require more sophisticated techniques, such as Bayesian optimization [45], [52], [63], [67], [69], [70], reinforcement learning [26], [67], or genetic algorithms [26], [40]. Recent work uses algorithms, such as stochastic gradient descent, that optimize a differentiable data-driven proxy model [13], [22], [23], [34].

None of these tools perform RTL simulation in the optimization loop. Instead, they evaluate designs with a performance model, and the final designs are evaluated with RTL simulation [13], [22], [31], [34], [69]. But inaccuracies in the performance model lead to suboptimal designs after they

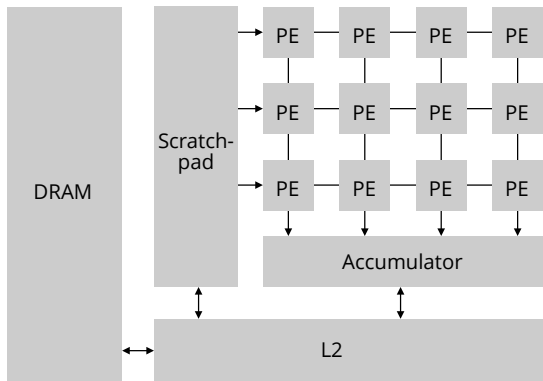


Fig. 2: A typical deep learning accelerator. Data is tiled in the scratchpad and fed into processing elements (PEs), which compute a convolution operation, using the accumulator to aggregate partial results.

are translated to hardware. Polaris avoids this inaccuracy by performing RTL simulation in the optimization loop.

III. BACKGROUND

This section provides background material that is useful for understanding our solution. We first provide an overview of deep learning workloads and deep learning accelerators. We then explain Bayesian optimization (BO), which is central to Polaris, before describing three relevant machine learning techniques, namely, variational autoencoders, deep kernel learning, and transfer learning.

A. Deep Learning Workloads and Accelerators

Deep learning (DL) models consist of a series of layers that can each be represented by a convolution operation,¹ so they are common targets for acceleration. A convolution is an operation on K weight tensors of size $R \times S \times C$ and N input tensors of size $(P + R - 1) \times (Q + S - 1) \times C$ to produce N output tensors of size $P \times Q \times K$. The convolution is implemented as a seven-level nested loop. Additional parameters of the convolution operation are the stride and dilation.

Deep learning accelerators (DLAs) execute the convolution operation on a spatial array of processing elements (PEs) connected to a specialized memory hierarchy that exploits the unique data reuse found in a convolution [6]. Figure 2 shows the primary components of the DLA we use for this work, Gemmini [19]. The PEs compute a partial convolution operation and stores intermediate results in an on-chip memory structure called an accumulator. To compute an entire DL layer, Gemmini streams data from DRAM, an L2 cache, and a software-managed scratchpad.

The data movement is precisely dictated by a per-layer *software mapping*. Specifically, a software mapping describes (1) how each tensor is tiled to fit in the memory hierarchy and (2) the order of the nested loops.

¹A convolution operation can represent a matrix multiply (GEMM) operation without loss of generality.

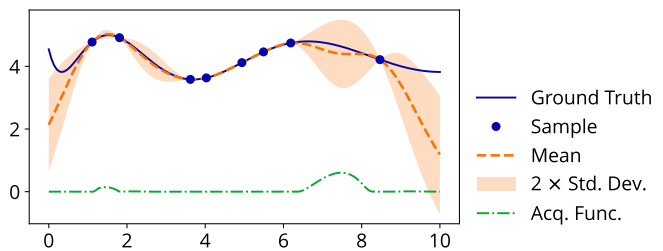


Fig. 3: A Gaussian process that models a ground truth function that has been sampled at 8 points. The acquisition function—in this case, Expected Improvement—is applied over the Gaussian process and maximized to determine the next sample to evaluate.

B. Bayesian Optimization

Bayesian optimization (BO) is an optimization strategy that is commonly employed when the *objective function*—i.e., the function that is being optimized—is expensive to evaluate [5]. BO has been successfully applied to perform DSE of the hardware/software (HW/SW) co-design space of DLAs [45], [48], [52], [63], [67], [70]. A BO framework consists of (1) a *surrogate model*, which cheaply predicts the value of the objective function, and (2) an *acquisition function*, which selects the next sample that should be evaluated.

The surrogate model is a data-driven model that must maintain a reliable measurement of uncertainty for its predictions—i.e., the output is a probability distribution rather than a single prediction. The most common type of surrogate model for BO is a Gaussian process (GP) [18], which produces a Gaussian distribution for a given input. Figure 3 shows a GP (shaded region and dashed line in orange) that is modeling a function (solid line in blue) given 8 samples. The shaded region represents the uncertainty of the surrogate model at any given input.

The acquisition function is a function that is applied over the surrogate model to balance exploration of uncertain regions with exploitation of the regions that are likely to contain the optimum. A common acquisition function is Expected Improvement (EI), which measures, as a function of every possible input, the change in expected value of the surrogate model. The acquisition function is maximized to select the next sample that should be evaluated. Figure 3 shows the EI acquisition function (dot-dash line in green) applied to the example GP. The acquisition function is maximized around $x = 7.5$, which is a region of high uncertainty. After evaluating that point, the acquisition function will be maximized around $x = 1.5$, which is the maximum of the ground truth.

Given the surrogate model and acquisition function, BO repeatedly performs the following operations, either for a fixed number of iterations or until a stopping criterion is met: (1) Select a sample by maximizing the acquisition function, (2) evaluate the sample on the expensive objective function, and (3) train the surrogate model with the new evaluation.

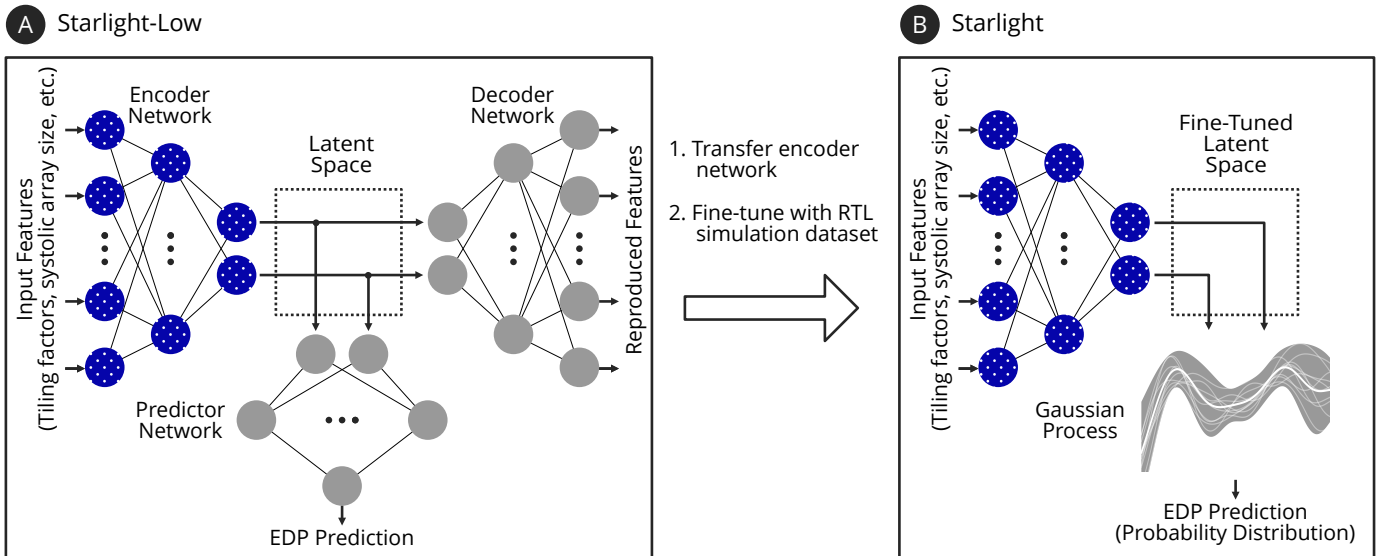


Fig. 4: **A** Starlight-Low is a neural network that predicts the energy-delay product (EDP) of a DLA as measured by a low-fidelity method, namely, an analytical model. The encoder network (in blue dotted pattern) from Starlight-Low is transferred to **B** Starlight, which is a machine learning model based on deep kernel learning that predicts the EDP as measured by a high-fidelity method, namely, an RTL simulator. The decoder network is dropped because it is no longer needed.

C. Machine Learning Techniques to Predict Performance

The traditional method of evaluating hardware is through the combined use of analytical models [35], [46], [54], timing simulators [44], [66], and RTL simulators [27], but recently a variety of machine learning techniques have been used to predict the performance of DLAs [13], [22], [32], [34]. Two techniques that have shown promising results [2], [23] are autoencoders [30], [49] and deep kernel learning [64].

An autoencoder [51] is a type of DL model that learns to compress with minimal loss a high-dimensional input into a low-dimensional space called a *latent space*. The architecture of an autoencoder is shown in the top part of Figure 4 **A**. On the left side of the autoencoder, in what is called the encoder network, is a series of fully-connected layers that decrease in size until they reach the target dimension of the latent space. On the right side of the autoencoder, in what is called the decoder network, is a series of fully-connected layers that mirrors the architecture of the encoder network. The autoencoder is trained to minimize the loss between the input of the encoder network and the output of the decoder network, which should precisely reconstruct the original input. Consequently, the autoencoder learns to encode inputs into unique representations in the low-dimensional latent space.

To avoid overfitting [4], we can inject randomness into the latent representations. Specifically, the last layer of the encoder network is modified to output a Gaussian distribution—as opposed to a scalar value—that non-deterministically encodes an input into the latent space. These so-called variational autoencoders (VAEs) [30] are widely accepted to be more robust than standard autoencoders.

Autoencoders and VAEs can accurately predict the performance of a DLA, and they can be trained with transfer learning

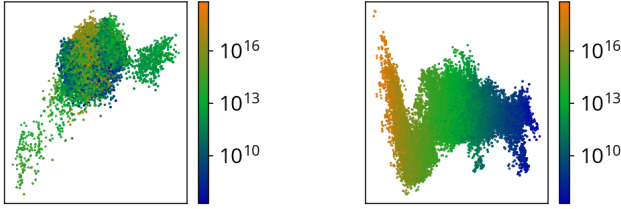
(Section III-D), but they are not suitable for use within a BO framework alone because they do not provide a reliable measurement of uncertainty. By contrast, Gaussian processes (GPs) do provide a reliable measurement of uncertainty, but GPs struggle to make predictions from high-dimensional input spaces such as the HW/SW co-design space [52]. To build a model that is suitable for BO—which is our intended use case for Starlight—we employ a recent technique from prior work called deep kernel learning (DKL) [3], [16], [38], [65]. DKL attaches an encoder network from a VAE to a Gaussian process (GP) to overcome limitations of the individual techniques: The encoder network reduces the dimensionality of the input space, and the GP provides a reliable measurement of uncertainty.

D. Transfer Learning

Transfer learning is a machine learning training technique that re-uses a model for a different task than it was originally trained for. There are many forms of transfer learning [71], but we focus on a straightforward form called hard weight sharing that directly transfers some trained weights from a *source model* to an untrained *target model*.

IV. STARLIGHT

In this section, we first present Starlight’s inputs and outputs and the dataset used for training. We then show that transfer learning can be applied to HW/SW co-design, and we present the source model, Starlight-Low, used to transfer knowledge to Starlight. Finally, we present Starlight, which is an accurate performance estimator that predicts the energy-delay product (EDP) of a DLA as measured by RTL simulation.



(a) Without predictor network. (b) With predictor network.

Fig. 5: The 2-D latent space of a VAE trained (a) without a predictor network and (b) simultaneously with a predictor network. Each point represents a HW/SW configuration that is color-coded by the EDP as measured by an analytical model. The predictor network induces structure, as indicated by the gradient of EDPs in the latent space.

Parameter	Values
Spatial Array Dimensions	4x4, 8x8, 16x16, 32x32
Accumulator Size	8 to 256 KB (Step Size: 8)
Scratchpad Size	8 to 256 KB (Step Size: 8)
Loop Order	Permutations of outermost loops
Tiling Factors [†]	Divisors of layer shape

[†]Independent values per level of memory hierarchy.

TABLE I: The ranges of parameter values in the input space of Starlight.

A. Inputs and Outputs

The inputs to Starlight-Low and Starlight are (1) the architectural parameters of a DLA and (2) the software mapping of a single convolutional layer. The output of Starlight is a Gaussian distribution that predicts energy-delay product (EDP) such that the mean represents the prediction and the standard deviation represents the uncertainty.

The precise hardware and software design space that Starlight-Low and Starlight are trained on is shown in Table I. In the hardware design space, both models accept as input the spatial array size and the accumulator and scratchpad sizes. In the software design space, both models accept as input the loop order and tiling factors. The loop order is encoded as a numerical value from 0 to 6 for each of the seven loops in the convolutional layer loop nest. All inputs are scaled to the range $[0, 1]$ using a min-max scaler.

B. Dataset

To train Starlight-Low, we collect a dataset of samples from the popular Timeloop analytical model [46], and to train Starlight, and we collect a dataset of samples from the FireSim RTL simulator [27]. The datasets are collected by performing Sobol sampling [59] cut for space: —a sampling method that results in a balanced dataset [13]—on the input space. We collect a total of 2^{16} samples from Timeloop and 2^{12} samples from FireSim.

We use both Timeloop and FireSim to measure the performance of the Gemmini DLA [19] when executing individual layers from one of four DL models (see Section VII).

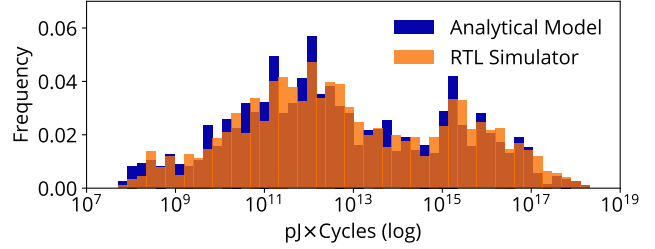


Fig. 6: The distribution of EDPs for the same 2^{12} HW/SW configurations as measured by an analytical model and by an RTL simulator. The similarity of the distributions indicates that knowledge can be transferred between models.

A limitation of our training data, and consequently of Starlight, is that FireSim does not measure energy consumption, so like prior work [22], we measure energy consumption using Timeloop. For the remainder of this paper, EDP refers to the product of energy consumption as measured by Timeloop and delay as measured by FireSim.²

C. Applicability of Transfer Learning

Transfer learning can be applied when the information used to predict one task can be transferred to the prediction of a different task. To measure the transferability of information between the Timeloop and FireSim datasets. Figure 6 shows the two distributions of EDPs. We compute the Kullback-Leibler (KL) divergence [33]—a common metric to measure distribution similarity (lower means more similar). For the overall distribution, the KL divergence is 0.04, indicating that information can be transferred. Furthermore, the KL divergence of the designs with the lowest 10% of EDPs—i.e., the key designs for design space exploration—is 0.12, indicating that there is information in the target distribution that a transferred model must learn to predict.

D. Starlight-Low

Starlight-Low is a neural network that predicts the EDP of Gemmini as measured by a low-fidelity method, namely, Timeloop [46]. Starlight-Low is used as the source model to transfer weights to Starlight.

The model architecture for Starlight-Low is based on a variational autoencoder (VAE) because VAEs reduce the dimensionality of the inputs, which is important when we incorporate a Gaussian process in Section IV-E. Traditionally, a VAE connects an encoder network to a symmetric decoder network and is trained to make the output reproduce the input exactly. We build and train a traditional VAE that encodes inputs into a 2-D latent space, which is shown in Figure 5a. Each point represents a HW/SW configuration, and the color indicates the EDP as measured by an analytical model. There

²To ensure the shared energy consumption measurement from Timeloop is not contaminating Starlight, we reproduce all experiments using only delay measurements, which are independently measured by Timeloop and FireSim. The behavior is identical to the experiments that use EDP.

is no apparent structure to the latent space, which indicates that the encoder is not properly learning the semantics of the inputs. Consequently, the latent space cannot reliably be used to make EDP predictions.

To induce structure in the latent space, as shown by the smooth gradient of EDPs in Figure 5b, prior work [20], [23] simultaneously trains a predictor network alongside the encoder and decoder networks. Figure 4 **A** shows the model architecture of Starlight-Low, which implements this technique. The inputs are encoded into the latent space and then fed to two outputs: the predictor network, which predicts the EDP of the configuration, and the decoder network, which reproduces the inputs to ensure that significant information is not lost in the latent space.

The final architecture of Starlight-Low is precisely as follows. The encoder network comprises fully connected layers of sizes 40, 24, 12, and 2, and the decoder network mirrors the encoder network. The predictor network comprises fully connected layers of sizes 2, 64, 256, 256, 64, and 1. In all cases, layers are fed through a ReLU activation function.

Starlight-Low is trained to minimize (1) the mean squared error between the predicted EDP and ground truth EDP, (2) the mean squared error between the reproduced inputs and actual inputs, and (3) the KL divergence between the latent encoding and unit multivariate Gaussian distribution. Minimizing KL divergence is the standard approach to ensure that the VAE does not collapse to a traditional autoencoder during training.

E. Starlight

Starlight is a machine learning model that predicts the EDP of a DLA as measured by a high-fidelity method, namely, an RTL simulator. Because Starlight is designed for use within a Bayesian optimization (BO) framework, it must provide a reliable measurement of uncertainty. To achieve this, we build Starlight using a technique called deep kernel learning [64] that fuses a neural network (which does not provide the measurement of uncertainty) with a Gaussian process (does provide the measurement of uncertainty).

To transfer knowledge from Starlight-Low to Starlight, we directly transfer the weights from the encoder network of Starlight-Low. We then fine-tune Starlight using a dataset of EDPs as measured by RTL simulation. We empirically validate this application of transfer learning in Section VII-A2.

To build Starlight, we modify the architecture of Starlight-Low in two key ways.

First, we remove the decoder network, because its goal is to prevent information loss in the latent space, but the encoder network that is transferred from Starlight-Low to Starlight already produces a well-behaved latent space.

Second, we replace the predictor network in Starlight-Low with a Gaussian process (GP). This neural model architecture, which ties together a neural network and a GP, is known as deep kernel learning (DKL) and is essential for enabling Starlight to be used as a surrogate model for a BO framework. DKL lends two additional benefits: (1) unlike a standalone GP, which is the typical surrogate model for a BO framework,

DKL supports transfer learning, and (2) DKL trains more robustly than other approaches, as shown in Section VII-A2.

The final architecture of Starlight is shown in Figure 4 **B**. The GP in Starlight uses a Matérn kernel [42] and gamma prior. To train Starlight, we maximize the marginal log likelihood of the combined encoder and GP [64].

V. POLARIS

Polaris is a Bayesian optimization (BO) framework built around Starlight that explores the co-design space of DLA design parameters and software mappings. Specifically, the inputs to Polaris are the shapes of the convolutional layers to be optimized; the outputs are the (1) architectural parameters for a DLA and (2) software mappings that minimize the energy-delay product (EDP) measured by RTL simulation. Polaris uses Starlight as its surrogate model, and it uses Upper Confidence Bound [60] as its acquisition function.

In this section, we first describe Polaris’ iterative HW-SW design process. We then describe the HW and SW optimizers.

A. Iterative Hardware-Software Design

It is challenging for a HW/SW co-design tool to simultaneously co-design both the hardware design and software mappings for all layers of a model because the co-design space is enormous: It is the Cartesian product of all hardware and software design parameters, e.g., $O(10^{140})$ for ResNet-50, which is a neural network used for image classification. Thus, similar to prior work [23], [40], [52], [63], [67], [70], Polaris is built using an iterative approach; it first selects a hardware candidate, then it optimizes each layer individually to find a software mapping that minimizes the EDP of running that layer on the selected hardware candidate. Figure 7 shows an overview of our approach.

B. Hardware Optimizer

The first step in an iteration of optimization with Polaris is to select a hardware candidate. In a traditional Bayesian optimizer (Section III-B), the acquisition function is maximized to select a candidate. However, the result is a value in a continuous input space, while the hardware design space is discrete. So Polaris instead enumerates the entire discrete hardware design space of $8 \times 32 \times 32$ designs defined in Table I, and then Polaris selects the candidate that maximizes the value of the acquisition function. Figure 7 shows this process; **H1** shows with shapes the candidates in the hardware design space, and **H2** shows the candidates being assessed by the acquisition function. The candidate that maximizes the acquisition function is shown with a filled circle, and it is fed as input to the software optimizer. The hardware optimization process is repeated for n iterations.

C. Layerwise Software Optimizer

Given a hardware candidate, the layerwise software optimizer finds optimized software mappings layer-by-layer. The process is similar to that of the hardware optimizer.

The first step is to select a software candidate. Because the software design space defined in Table I is much larger

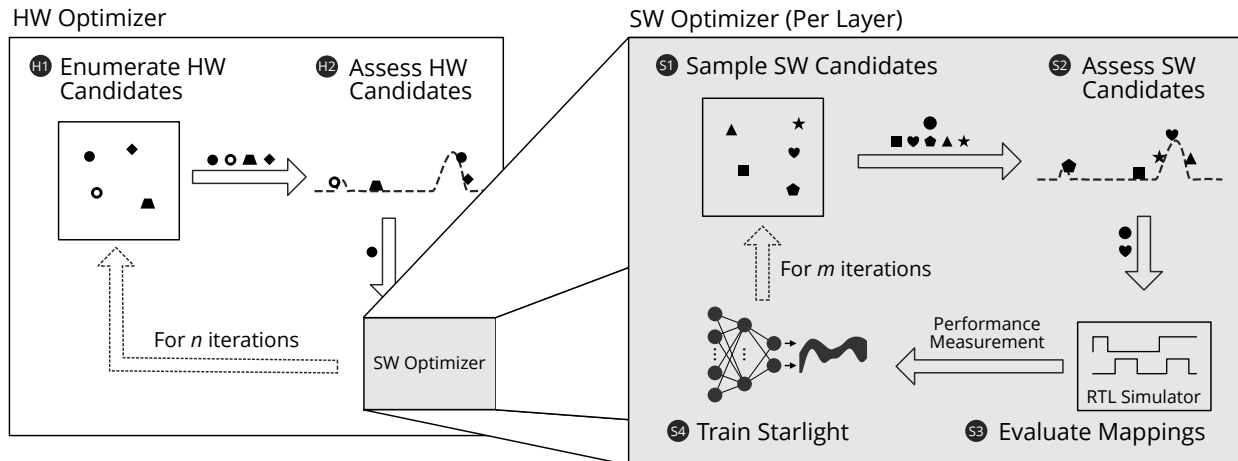


Fig. 7: Polaris is a DSE tool that takes as input layer shapes that define the workload to be optimized and outputs an optimized DLA and software mappings. The optimizer is split into an outer loop to optimize hardware and an inner loop to optimize software. The sequence of operations is as follows. A hardware candidate is selected (**H1**) and rounded to the nearest—as measured by distance in the latent space—implementable configurations (**H2**). Then, software candidates are selected for every layer (**S1**) and rounded to the nearest implementable configurations (**S2**) before being evaluated with an RTL simulator (**S3**). Finally, Starlight is updated with the new evaluations (**S4**). The process repeats for n trials in the hardware optimizer and m trials in the software optimizer.

than the hardware design space, it is infeasible to evaluate the acquisition function for every software design. To reduce the number of designs without deteriorating their quality, we enforce three reasonable constraints: (1) the designs must be implementable on the selected hardware candidate, (2) the spatially unrolled dimensions—the C and K dimensions for Gemmini—should maximize the utilization of the hardware, and (3) the tiling factors should evenly divide the shape of the layer so that there are no extraneous edge cases that increase the tail latency when running the layer. Even after applying these constraints, the software design space can still contain millions of points. Thus, Polaris selects a software candidate as follows: It randomly draws using a Sobol sequence 10,000 samples from the large, constrained software space, and it then assesses each of the candidates with the acquisition function, selecting the software candidate that maximizes the acquisition function. This process is shown in Figure 7 **S1** and **S2** . The software candidate that is selected is shown with a heart, and the hardware candidate selected by the hardware optimizer is still shown with a circle.

Once the HW/SW candidate is selected, it is evaluated on an RTL simulator, FireSim [27], as shown in **S3** , and Starlight is trained with the new evaluation, as shown in **S4** . The software optimization process repeats for m iterations.

VI. METHODOLOGY

This section presents our evaluation methodology. We first describe the DL models that we use to evaluate Starlight and Polaris. We then describe our methodology for evaluating each tool.

A. DL Models

We first train Starlight and Starlight-Low to predict the energy-delay product (EDP) of executing individual layers from the following set of diverse DL models. We then use Polaris to perform HW/SW co-design for each of these models independently.

- U-Net [50] is a large convolutional neural network (CNN) used for biomedical image segmentation.
- ResNet-50 [21] is a CNN used for image classification.
- BERT [9] is a transformer used for natural language processing.
- RetinaNet [39] is CNN that adds to ResNet-50 a feature pyramid network, classification head, and regression head. We only evaluate these added layers.

B. Starlight Methodology

We measure the accuracy of Starlight and Starlight-Low using Spearman rank correlation, ρ [17], which compares the relative ordering—as opposed to the precise value—of the predicted and ground truth measurements. ρ ranges from -1 to +1, where -1 means the relative orders are exactly reversed and +1 means the relative orders are identical. Because Starlight is used as the surrogate model of Polaris, it need not predict the absolute performance value with high accuracy; it is sufficient for it to have high positive ρ .³

Unless otherwise specified, we use 80% of the datasets described in Section IV-B for training and 20% for testing.

³For the sake of completion, we also measure the typical accuracy metric—co-relation coefficient—to be 97%.

C. Polaris Methodology

We compare Polaris against three baselines.

First, Offline Random draws random samples from the hardware and software design spaces and evaluates them on Starlight. The configuration that minimizes EDP as predicted by Starlight is evaluated using RTL simulation. By using Starlight for evaluation, Offline Random allows us to make a direct comparison between offline optimization—i.e., optimizing a proxy model without evaluating intermediate candidates using RTL simulation—and online optimization—i.e., performing optimization by evaluating intermediate candidates using RTL simulation. We use random optimization instead of optimization strategies such as stochastic gradient descent because the latter optimizes the proxy model in a continuous space, and we find that “snapping” the results to an implementable design in the discrete design space yields designs that are three orders of magnitude less performant than those produced by random optimization.

Second, DOSA [22] is a state-of-the-art HW/SW co-design tool that uses the same evaluation methodology as Polaris. DOSA performs stochastic gradient descent on a data-driven proxy model to find a HW/SW configuration that minimizes EDP as predicted by the proxy model. The resulting design is evaluated using RTL simulation. DOSA performs offline optimization on a smaller design space than Polaris: It does not explore the spatial array dimensions, and it only explores three possible loop orders. We address these limitations in Section VII-B2.

Third, Spotlight [52] is a state-of-the-art HW/SW co-design tool that performs a feature transformation to improve the sample-efficiency of a vanilla BO framework. We adapt the methodology used for Spotlight to evaluate candidates using RTL simulation in Polaris’ design space. Spotlight performs online optimization.

We evaluate our tools in two design scenarios. First, we perform HW/SW co-design as described previously. But since DOSA critically does not include the spatial array dimensions in its design space, we evaluate the baselines in a second design scenario: software DSE. When performing software DSE, we use the DLA designs found by DOSA and only perform layerwise software optimization.

When performing HW/SW co-design, Spotlight and Polaris run for $n = 8$, $m = 6$ iterations. For fairness, Offline Random draws $8 \times 6 \times 10000 = 480000$ samples per layer from the HW/SW co-design space (recall that Polaris evaluates 10,000 samples on the acquisition function per software iteration). When performing software DSE, Spotlight and Polaris run for $m = 20$ iterations, and Offline Random draws $20 \times 10000 = 200000$ samples per layer from the software design space. Polaris and Spotlight both run for three independent trials, and the median, minimum, and maximum of the trials are reported.

VII. EVALUATION

A. Starlight

This section evaluates Starlight’s accuracy and robustness.

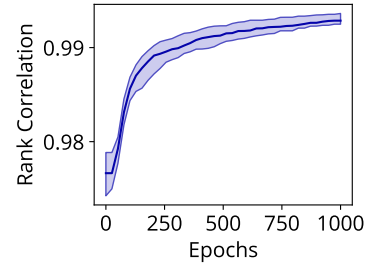


Fig. 8: Starlight predicts EDP measured by RTL simulation, with Spearman rank correlation (ρ) of 0.99 after 1000 epochs of training. Across 10 independent trials, Starlight consistently achieves a median ρ , shown with the solid line, of greater than 0.98 within 100 epochs. Furthermore, the narrowness of the shaded region, which denotes the cumulative minimum and maximum ρ across the 10 trials, shows that Starlight trains accurately irrespective of the specific partition of training data that is used. Higher is better.

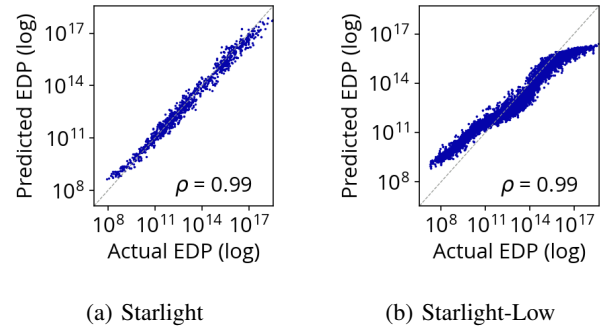


Fig. 9: Accuracy and Spearman rank correlation (ρ) of the actual EDP and the predicted EDP for (a) Starlight and (b) Starlight-Low. Perfect accuracy is $y = x$ and $\rho = 1$.

1) *Accuracy*: Figure 8 presents ρ during training. We perform 10 independent trials of training and plot the median (denoted by the central line) and cumulative minimum and maximum (denoted by the shaded region). Starlight achieves $\rho = 0.99$ after 1000 epochs of training (2 minutes of training time on a consumer-grade CPU), and it consistently achieves $\rho \geq 0.98$ after just 100 trials (13 seconds of training time on a consumer-grade CPU). Because the shaded region is narrow (standard deviation of 3.9×10^{-4}), we conclude that Starlight is not sensitive to the specific partition of the training data that is used. Note that the initial accuracy is already high, demonstrating that transfer learning provides significant benefit. We further investigate this claim in Section VII-A2.

Figures 9a and 9b show the accuracy and ρ for Starlight and Starlight-Low, respectively. The X axis shows the ground truth EDP measured by either FireSim for Starlight or by Timeloop for Starlight-Low, and the Y axis shows the predicted EDP. Each dot represents a sample from the test set. If a sample is predicted with perfect accuracy, it aligns with $y = x$.

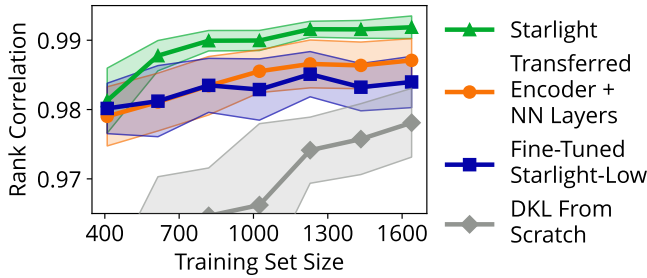


Fig. 10: ρ versus the FireSim training set size. We evaluate four model architectures: (1) Starlight, (2) a neural network that leverages transfer learning, (3) a simple fine-tuning of Starlight-Low, and (4) a DKL trained from scratch. The solid line indicates the mean of ten trials, and the shaded region indicates one standard deviation. Starlight consistently achieves the highest ρ and is more resilient to the training set size and partition than other models. Higher is better.

Both Starlight and Starlight-Low achieve high accuracy—as is indicated by the average distance across samples from $y = x$ —and a ρ of 0.99.

Key Takeaway: Starlight achieves high accuracy when predicting EDP as measured by RTL simulation.

2) *Robustness:* Starlight achieves higher accuracy than Starlight-Low on their respective datasets. By comparing against three other performance estimation approaches, we show, that Starlight’s high accuracy can be attributed to the use of both transfer learning and deep kernel learning (DKL). First, we compare against a model based on DKL with the same architecture as Starlight but that is trained from scratch (DKL From Scratch). We then compare against a model that employs transfer learning but trains a neural network predictor rather than a model based on DKL (Transferred Encoder + NN Layers). Finally, we compare against a simple fine-tuning of the source model, Starlight-Low, that is trained without the use of transfer learning (Fine-Tuned Starlight-Low).

Each model is trained with a range of training set sizes, and the training process and the partitioning of the training set are repeated for 10 independent trials. Figure 10 shows the results. The X axis shows the number of samples in the training set, and the Y axis shows ρ when each model predicts EDP of the test set. The solid line indicates the mean of the trials, and the shaded region indicates 1 standard deviation across the trials.

Starlight consistently achieves the highest ρ out of the evaluated models, irrespective of training set size. Furthermore, Starlight achieves the smallest standard deviation across trials, indicating that it is the most robust of the evaluated models.

When trained on the full training set, DKL From Scratch achieves a mean of $\rho = 0.973$. Although this is high, it is significantly lower than the other models evaluated, and the accuracy quickly deteriorates if the training set size is reduced. Overall, DKL From Scratch consistently achieves the lowest accuracy. However, Starlight also employs a model based on DKL, so we conclude that DKL requires a large amount of

data, but it can be robust and achieve high accuracy.

To isolate the effects of transfer learning, we also compare against Transferred Encoder + NN Layers. This model achieves high accuracy, but Starlight consistently achieves higher accuracy, indicating that transfer learning is beneficial. But DKL gives Starlight an edge over other approaches.

Finally, to further validate our use of transfer learning, We compare against Fine-Tuned Starlight-Low. This model achieves high accuracy, but Starlight and Transferred Encoder + NN Layers both consistently achieve higher accuracy.

Key Takeaway: Both DKL and transfer learning are instrumental to Starlight’s high accuracy and robustness.

B. Polaris

In this section, we first demonstrate Polaris’ advantage over prior work when performing HW/SW co-design and software DSE. We then compare the behavior of our online methods: Spotlight and Polaris.

1) *HW/SW Co-Design:* Figure 11 compares the EDP of the designs produced by Offline Random, DOSA, Spotlight, and Polaris when performing HW/SW co-design. The bars indicate the median of 3 independent trials, and the error bars indicate the minimum and maximum of the trials.

In the median, Polaris consistently produces designs with the lowest EDP, and Spotlight always produces designs that achieve lower EDP than those produced by DOSA. Part of this success can be attributed to the selection of spatial array size, which is a design parameter that greatly affects EDP and that is not explored by DOSA. In particular, the 32×32 spatial array is almost always selected by Polaris and Spotlight because it reduces EDP. In the outlying maximum trial of ResNet-50, Polaris does not select a 32×32 spatial array. Similarly, DOSA always uses a 16×16 spatial array, so it achieves higher EDP than Polaris and Spotlight. However, the spatial array size is not the sole reason for Polaris’ success; Offline Random always selects a 32×32 spatial array, but it is unable to select other commensurate design parameter values, so its designs always result in higher EDP than both Spotlight and Polaris.

Key Takeaway: The online methods, Polaris and Spotlight, consistently produce designs with lower EDP than the offline methods when performing HW/SW co-design, and Polaris consistently produces designs with the lowest median EDP.

2) *Software DSE:* Because the DLA architecture significantly affects the final EDP found, we select a fixed DLA design—specifically, the DLA design selected by DOSA—and only perform software DSE to produce software mappings. Figure 12 summarizes these results.

We again find that Polaris consistently produces designs that achieve the lowest EDP, but its improvement over the baselines is smaller. Furthermore, the EDP achieved when Polaris performs software DSE is consistently higher than the EDP achieved when Polaris performs HW/SW co-design. These results corroborate prior work [46], [57] that highlights the importance of performing HW/SW co-design.

We also find that Spotlight no longer consistently produces software mappings with lower EDP than those produced by

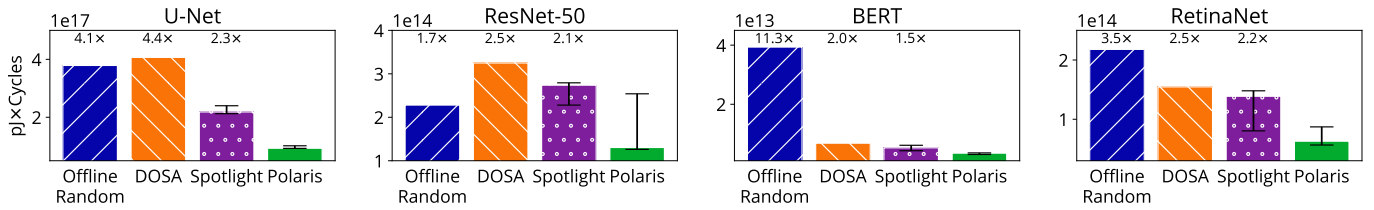


Fig. 11: We compare the best designs produced by Offline Random, DOSA, Spotlight, and Polaris when performing HW/SW co-design to minimize EDP. Lower is better.

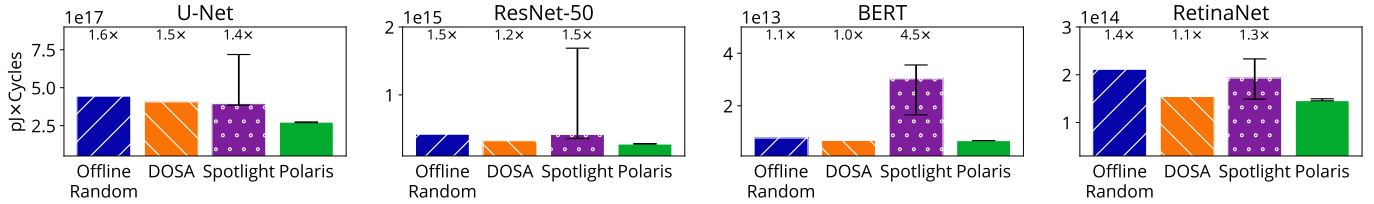


Fig. 12: We compare the best software mappings produced by Offline, DOSA, Spotlight, and Polaris when performing software DSE to minimize EDP on the DLA design selected by DOSA. Lower is better.

DOSA, and the variance across trials is significantly higher. We hypothesize that Spotlight, which is trained from scratch on each trial, struggles to learn the characteristics of the design space when it has fewer degrees of freedom to learn from. On the other hand, Polaris’s proxy model, Starlight, is already trained on the design space and can navigate it effectively from the start.

Key Takeaway: Polaris consistently produces software mappings that achieve lower EDP than the baselines when performing software DSE, and in general it is important to perform HW/SW co-design when designing DLAs.

3) *Online Optimization Behavior:* Figure 13 summarizes our investigation into the behavior of online optimization. The X axis shows the overall iteration of the hardware and software optimizers, and the gray dashed lines demarcate the 8 hardware candidates that are evaluated. The Y axis shows the cumulative minimum EDP that has been achieved thus far. For Polaris and Spotlight, the solid line indicates the median of 3 independent trials, and the shaded region indicates the minimum and maximum across the trials.

For U-Net, ResNet-50, and BERT, Polaris’ optimization quickly converge, whereas Spotlight’s optimization is more segmented. This behavior is unsurprising because Polaris is trained on a dataset of RTL simulations, so it begins the optimization with a noteworthy head-start. Spotlight begins with 3 uniformly random samples to seed the surrogate model, and it continues to learn the shape of the design space to reduce its achieved EDP. If given more iterations, Spotlight may eventually produce results similar to Polaris’s, but we explain in Section VII-C why Polaris is still a better choice for HW/SW co-design when the evaluation method is slow.

Finally, across all models and for both Polaris and Spotlight, the biggest changes in EDP occur when a new hardware candidate is selected—i.e., at the grey dashed lines. Thus, we

Model	HW/SW Co-Design		SW DSE	
	Spotlight	Polaris	Spotlight	Polaris
U-Net	9.19h	0.35h	2.28h	0.31h
ResNet-50	1.70h	0.29h	-	0.44h
BERT	0.98h	0.10h	-	0.39h
RetinaNet	1.37h	1.60h	0.41h	0.92h

TABLE II: The wall-clock time for each online method—when performing HW/SW co-design and software DSE—to produce designs that achieve lower EDP than the designs found by DOSA. Lower is better.

see that the choice of hardware candidate plays a significant role in the final achievable EDP, but the software mappings must properly optimized for the hardware.

We perform this same analysis for software DSE, but we omit the results for brevity because they are similar to that of HW/SW co-design.

Key Takeaway: Polaris and Spotlight both find designs with low EDP when performing HW/SW co-design, but Polaris is more sample-efficient. Furthermore, the choice of hardware candidate plays a significant role in the final achievable EDP.

C. Discussion

Offline Random and DOSA both perform offline optimization, while Spotlight and Polaris both perform online optimization. Figures 11 and 12 both clearly illustrate the benefit of performing online optimization: The online methods can produce better designs than the offline methods.

Another important metric to compare the quality of these tools is the amount of wall-clock time it takes for the online methods to outperform the offline methods. Table II presents these results. Within a maximum of 1.6 hours and an average of 35 minutes, Polaris always produces designs that outperform those produced by DOSA in 6 hours, and the remainder

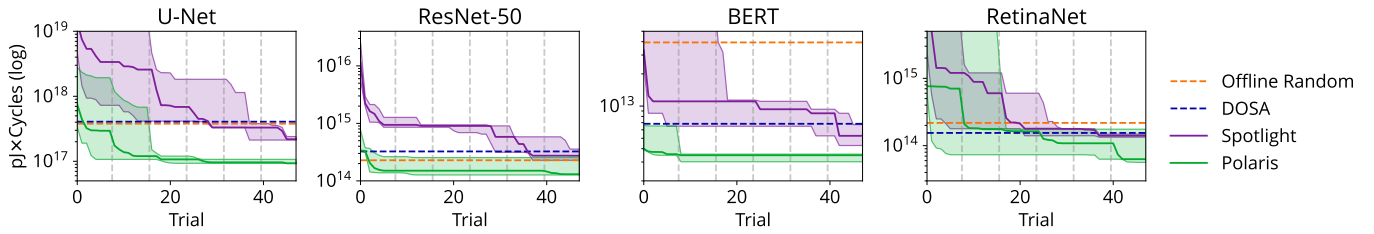


Fig. 13: The behavior Polaris and Spotlight when performing HW/SW co-design. Each segment demarcated by a gray dashed line is a single hardware candidate, and the solid line indicates the cumulative minimum EDP found thus far. Lower is better.

of the time is spent exploring designs that achieve even lower EDP. And because intermediate designs are evaluated using RTL simulation, both Polaris and Spotlight continuously learn more about the design space and will likely continue to reduce EDP with each iteration.

Polaris is generally faster than Spotlight at producing designs that outperform those produced by DOSA. There are two reasons for this. First, Polaris is warmed up with the dataset of RTL simulations, so it is able to quickly find designs that achieve low EDP. Second, the RTL simulations for Polaris’ candidate designs have shorter wall-clock time than that of Spotlight’s candidate designs because the wall-clock time of RTL simulation is correlated with the delay of the design being simulated, and Spotlight’s designs typically have higher delay.

Of course, Polaris requires a dataset of Timeloop evaluations and RTL simulations to be collected beforehand, which incurs an 8-hour, one-time cost that Spotlight does not incur. However, in practice, Polaris will be run multiple times over the course of the DLA development cycle, so the cost of collecting the dataset is amortized. Over time, Polaris provides significantly higher sample-efficiency than Spotlight, so it is the better choice for HW/SW co-design when the evaluation method is slow.

Polaris achieves its high sample-efficiency by spending more wall-clock time than Spotlight to select candidates to evaluate using RTL simulation. But in situations where the evaluation method is fast, such as early in the development cycle when designs are evaluated using an analytical model, approaches like Spotlight may be better suited because they can evaluate a larger number of candidates.

VIII. CONCLUSIONS

In this paper, we have shown that transfer learning can be effectively employed to transfer knowledge from a low-fidelity performance model to a high-fidelity performance model. In particular, we have shown that a data-driven model that has been trained using a fast analytical model can reduce the number of slow evaluations needed to train a high-fidelity data-driven model. Our resulting data-driven model can be queried faster than an analytical model and can achieve 99% accuracy when predicting the EDP of a DLA. Moreover, Starlight is trained with 61% fewer high-fidelity evaluations and achieves higher accuracy than DOSA’s state-of-the-art data-driven model [22].

We have also used Starlight as a key component in Polaris, which is the first DSE tool that performs RTL simulation in the optimization loop. Polaris produces designs that reduce the energy-delay product by $2.7\times$ over DOSA and by $5.15\times$ over an ablated version of Polaris that does not perform RTL simulation in the optimization loop.

The methodology that we have presented in this paper may be applicable to other areas of hardware design in general where there is close similarity between low-fidelity evaluation methods and high-fidelity evaluation methods and where high-fidelity evaluation methods are slow. Irrespective of its broader applicability, our methodology indicates the importance of exploiting properties of the problem—e.g., the transferability of knowledge between low and high fidelity performance models—to design customized design space exploration tools.

REFERENCES

- [1] D. Abts, I. Ahmed, A. Bitar, M. Boyd, J. Kim, G. Kimmell, and A. Ling, “Challenges/Opportunities to Enable Dependable Scale-out System with Groq Deterministic Tensor-Streaming Processors,” in *Dependable Systems and Networks (DSN-S)*, Jun. 2022.
- [2] C. Bai, Q. Sun, J. Zhai, Y. Ma, B. Yu, and M. D. Wong, “BOOM-Explorer: RISC-V BOOM Microarchitecture Design Space Exploration Framework,” in *International Conference On Computer-Aided Design (ICCAD)*, Nov. 2021.
- [3] T. Bai, Y. Li, Y. Shen, X. Zhang, W. Zhang, and B. Cui, “Transfer Learning for Bayesian Optimization: A Survey,” *arXiv*, Feb. 2023.
- [4] D. Bank, N. Koenigstein, and R. Giryes, “Autoencoders,” in *Data Mining and Knowledge Discovery Handbook*, L. Rokach, O. Maimon, and E. Shmueli, Eds., 2023.
- [5] B. Bischl, M. Binder, M. Lang, T. Pielok, J. Richter, S. Coors, J. Thomas, T. Ullmann, M. Becker, A.-L. Boulesteix, D. Deng, and M. Lindauer, “Hyperparameter Optimization: Foundations, Algorithms, Best Practices, and Open Challenges,” *WIREs Data Mining and Knowledge Discovery*, no. 2, 2023.
- [6] Y.-H. Chen, T. Krishna, J. S. Emer, and V. Sze, “Eyeriss: An Energy-Efficient Reconfigurable Accelerator for Deep Convolutional Neural Networks,” *Solid-State Circuits*, no. 1, Jan. 2017.
- [7] Y.-H. Chen, T.-J. Yang, J. Emer, and V. Sze, “Eyeriss v2: A Flexible Accelerator for Emerging Deep Neural Networks on Mobile Devices,” *Emerging and Selected Topics in Circuits and Systems*, no. 2, Jun. 2019.
- [8] S. Dave, Y. Kim, S. Avancha, K. Lee, and A. Shrivastava, “dMazeRunner: Executing Perfectly Nested Loops on Dataflow Accelerators,” *Transactions on Embedded Computing Systems*, no. 5s, Oct. 2019.
- [9] J. Devlin, M.-W. Chang, K. Lee, and K. Toutanova, “BERT: Pre-training of Deep Bidirectional Transformers for Language Understanding,” *arXiv*, May 2019.
- [10] P. Dhillewararao, S. Boppu, M. S. Manikandan, and L. R. Cenkermaddi, “Efficient Hardware Architectures for Accelerating Deep Neural Networks: Survey,” *IEEE Access*, 2022.
- [11] S. Dong, P. Wang, and K. Abbas, “A Survey on Deep Learning and Its Applications,” *Computer Science Review*, 2021.

- [12] M. Emani, V. Vishwanath, C. Adams, M. E. Papka, R. Stevens, L. Florescu, S. Jairath, W. Liu, T. Nama, and A. Sajeeth, "Accelerating Scientific Applications With SambaNova Reconfigurable Dataflow Architecture," *Computing in Science & Engineering*, no. 2, Mar. 2021.
- [13] H. Esmailzadeh, S. Ghodrati, A. B. Kahng, J. K. Kim, S. Kinzer, S. Kundu, R. Mahapatra, S. D. Manasi, S. Sapatnekar, Z. Wang, and Z. Zeng, "An Open-Source ML-Based Full-Stack Optimization Framework for Machine Learning Accelerators," *arXiv*, Aug. 2023.
- [14] H. Esmailzadeh, S. Ghodrati, A. B. Kahng, J. K. Kim, S. Kinzer, S. Kundu, R. Mahapatra, S. D. Manasi, S. S. Sapatnekar, Z. Wang, and Z. Zeng, "Physically Accurate Learning-Based Performance Prediction of Hardware-Accelerated ML Algorithms," in *Workshop on Machine Learning for CAD (MLCAD)*, Sep. 2022.
- [15] M. Ferianc, H. Fan, D. Manocha, H. Zhou, S. Liu, X. Niu, and W. Luk, "Improving Performance Estimation for Design Space Exploration for Convolutional Neural Network Accelerators," *Electronics*, no. 4, Jan. 2021.
- [16] M. Feurer, B. Letham, F. Hutter, and E. Bakshy, "Practical Transfer Learning for Bayesian Optimization," *arXiv*, Oct. 2022.
- [17] E. C. Fieller, H. O. Hartley, and E. S. Pearson, "Tests for Rank Correlation Coefficients, I," *Biometrika*, no. 3-4, Dec. 1957.
- [18] A. I. Forrester, A. Söbester, and A. J. Keane, "Multi-fidelity Optimization via Surrogate Modelling," *Royal Society A: Mathematical, Physical and Engineering Sciences*, no. 2088, Oct. 2007.
- [19] H. Genc, S. Kim, A. Amid, A. Haj-Ali, V. Iyer, P. Prakash, J. Zhao, D. Grubb, H. Liew, H. Mao, A. Ou, C. Schmidt, S. Steffl, J. Wright, I. Stoica, J. Ragan-Kelley, K. Asanovic, B. Nikolic, and Y. S. Shao, "Gemmini: Enabling Systematic Deep-Learning Architecture Evaluation via Full-Stack Integration," in *Design Automation Conference (DAC)*, Dec. 2021.
- [20] R. Gómez-Bombarelli, J. N. Wei, D. Duvenaud, J. M. Hernández-Lobato, B. Sánchez-Lengeling, D. Sheberla, J. Aguilera-Iparraguirre, T. D. Hirzel, R. P. Adams, and A. Aspuru-Guzik, "Automatic Chemical Design Using a Data-Driven Continuous Representation of Molecules," *ACS Central Science*, no. 2, Feb. 2018.
- [21] K. He, X. Zhang, S. Ren, and J. Sun, "Deep Residual Learning for Image Recognition," in *Computer Vision and Pattern Recognition (CVPR)*, 2016.
- [22] C. Hong, Q. Huang, G. Dinh, M. Subedar, and Y. S. Shao, "DOSA: Differentiable Model-Based One-Loop Search for DNN Accelerators," in *Microarchitecture (MICRO)*, Dec. 2023.
- [23] Q. Huang, C. Hong, J. Wawrzyniec, M. Subedar, and Y. S. Shao, "Learning A Continuous and Reconstructible Latent Space for Hardware Accelerator Design," in *International Symposium on Performance Analysis of Systems and Software (ISPASS)*, May 2022.
- [24] N. P. Jouppi, D. Hyun Yoon, M. Ashcraft, M. Gottscho, T. B. Jablin, G. Kurian, J. Laudon, S. Li, P. Ma, X. Ma, T. Norrie, N. Patil, S. Prasad, C. Young, Z. Zhou, and D. Patterson, "Ten Lessons From Three Generations Shaped Google's TPUv4i : Industrial Product," in *International Symposium on Computer Architecture (ISCA)*, Jun. 2021.
- [25] N. P. Jouppi, C. Young, N. Patil, D. Patterson, G. Agrawal, R. Bajwa, S. Bates, S. Bhatia, N. Boden, A. Borchers, R. Boyle, P.-I. Cantin, C. Chao, C. Clark, J. Coriell, M. Daley, M. Dau, J. Dean, B. Gelb, T. V. Ghaemmaghami, R. Gottipati, W. Gulland, R. Hagmann, C. R. Ho, D. Hogberg, J. Hu, R. Hundt, D. Hurt, J. Ibarz, A. Jaffey, A. Jaworski, A. Kaplan, H. Khaitan, D. Killebrew, A. Koch, N. Kumar, S. Lacy, J. Laudon, J. Law, D. Le, C. Leary, Z. Liu, K. Lucke, A. Lundin, G. MacKean, A. Maggiore, M. Mahony, K. Miller, R. Nagarajan, R. Narayanaswami, R. Ni, K. Nix, T. Norrie, M. Omernick, N. Penukonda, A. Phelps, J. Ross, M. Ross, A. Salek, E. Samadiani, C. Severn, G. Sizikov, M. Snellham, J. Souter, D. Steinberg, A. Swing, M. Tan, G. Thorson, B. Tian, H. Toma, E. Tuttle, V. Vasudevan, R. Walter, W. Wang, E. Wilcox, and D. H. Yoon, "In-Datcenter Performance Analysis of a Tensor Processing Unit," in *International Symposium on Computer Architecture (ISCA)*, Jun. 2017.
- [26] S.-C. Kao, G. Jeong, and T. Krishna, "ConfuciusX: Autonomous Hardware Resource Assignment for DNN Accelerators using Reinforcement Learning," in *Microarchitecture (MICRO)*, Oct. 2020.
- [27] S. Karandikar, H. Mao, D. Kim, D. Biancolin, A. Amid, D. Lee, N. Pemberton, E. Amaro, C. Schmidt, A. Chopra, Q. Huang, K. Kovacs, B. Nikolic, R. Katz, J. Bachrach, and K. Asanović, "Firesim: FPGA-Accelerated Cycle-Exact Scale-Out System Simulation in the Public Cloud," in *International Symposium on Computer Architecture (ISCA)*, Jun. 2018.
- [28] S. Kaufman, P. Phothilimthana, Y. Zhou, C. Mendis, S. Roy, A. Sabne, and M. Burrows, "A Learned Performance Model for Tensor Processing Units," in *Machine Learning and Systems*, A. Smola, A. Dimakis, and I. Stoica, Eds., 2021.
- [29] S. Kim, C. Hooper, T. Wattanawong, M. Kang, R. Yan, H. Genc, G. Dinh, Q. Huang, K. Keutzer, M. W. Mahoney, Y. S. Shao, and A. Gholami, "Full Stack Optimization of Transformer Inference: A Survey," *arXiv*, Feb. 2023.
- [30] D. P. Kingma and M. Welling, "Auto-Encoding Variational Bayes," *arXiv*, Dec. 2022.
- [31] D. Koeplinger, M. Feldman, R. Prabhakar, Y. Zhang, S. Hadjis, R. Fiszal, T. Zhao, L. Nardi, A. Pedram, C. Kozyrakis, and K. Olukotun, "Spatial: A language and compiler for application accelerators," in *Programming Language Design and Implementation (PLDI)*, Jun. 2018.
- [32] S. Krishnan, A. Yazdanbakhsh, S. Prakash, J. Jabbour, I. Uchendu, S. Ghosh, B. Boroujerdian, D. Richins, D. Tripathy, A. Faust, and V. Janapa Reddi, "ArchGym: An Open-Source Gymnasium for Machine Learning Assisted Architecture Design," in *International Symposium on Computer Architecture (ISCA)*, Jun. 2023.
- [33] S. Kullback and R. A. Leibler, "On Information and Sufficiency," *The Annals of Mathematical Statistics*, no. 1, 1951.
- [34] A. Kumar, A. Yazdanbakhsh, M. Hashemi, K. Swersky, and S. Levine, "Data-Driven Offline Optimization for Architecting Hardware Accelerators," in *International Conference on Learning Representations (ICLR)*, Oct. 2021.
- [35] H. Kwon, P. Chatarasi, V. Sarkar, T. Krishna, M. Pellauer, and A. Parashar, "MAESTRO: A Data-Centric Approach to Understand Reuse, Performance, and Hardware Cost of DNN Mappings," *IEEE Micro*, no. 3, May 2020.
- [36] C. Lattner, M. Amini, U. Bondhugula, A. Cohen, A. Davis, J. Pienaar, R. Riddle, T. Shpeisman, N. Vasilache, and O. Zinenko, "MLIR: Scaling Compiler Infrastructure for Domain Specific Computation," in *Code Generation and Optimization (CGO)*, Feb. 2021.
- [37] A. Lavelly, "Powering Extreme-Scale HPC with Cerebras Wafer-Scale Accelerators," Cerebras Systems, Inc, Tech. Rep., 2022.
- [38] Y. L. Li, T. G. J. Rudner, and A. G. Wilson, "A Study of Bayesian Neural Network Surrogates for Bayesian Optimization," *arXiv*, May 2023.
- [39] T.-Y. Lin, P. Goyal, R. Girshick, K. He, and P. Dollar, "Focal Loss for Dense Object Detection," in *International Conference on Computer Vision (ICCV)*, 2017.
- [40] Y. Lin, M. Yang, and S. Han, "NAAS: Neural Accelerator Architecture Search," in *Design Automation Conference (DAC)*, Dec. 2021.
- [41] N. Maslej, L. Fattorini, E. Brynjolfsson, J. Etchemendy, K. Ligett, T. Lyons, J. Manyika, H. Ngo, V. Parli, Y. Shoham, R. Wald, J. Clark, and R. Perrault, "The AI Index 2023 Annual Report," Institute for Human-Centered AI, Tech. Rep., Apr. 2023.
- [42] B. Matérn, *Spatial Variation*, D. Brillinger, S. Fienberg, J. Gani, J. Hartigan, and K. Krickeberg, Eds., 1986.
- [43] L. Mei, P. Houshmand, V. Jain, S. Giraldo, and M. Verhelst, "ZigZag: Enlarging Joint Architecture-Mapping Design Space Exploration for DNN Accelerators," *Transactions on Computers*, no. 8, Aug. 2021.
- [44] F. Muñoz-Martínez, J. L. Abellán, M. E. Acacio, and T. Krishna, "STONNE: Enabling Cycle-Level Microarchitectural Simulation for DNN Inference Accelerators," in *International Symposium on Workload Characterization (IISWC)*, Nov. 2021.
- [45] L. Nardi, D. Koeplinger, and K. Olukotun, "Practical Design Space Exploration," in *Modeling, Analysis, and Simulation of Computer and Telecommunication Systems (MASCOTS)*, Oct. 2019.
- [46] A. Parashar, P. Raina, Y. S. Shao, Y.-H. Chen, V. A. Ying, A. Mukkara, R. Venkatesan, B. Khailany, S. W. Keckler, and J. Emer, "Timeloop: A Systematic Approach to DNN Accelerator Evaluation," in *International Symposium on Performance Analysis of Systems and Software (ISPASS)*, Mar. 2019.
- [47] C. Pham-Quoc, X.-Q. Nguyen, and T. N. Think, "Hardware/Software Co-design for Convolutional Neural Networks Acceleration: A Survey and Open Issues," in *Context-Aware Systems and Applications*, P. Cong Vinh and A. Rakib, Eds., 2021.
- [48] B. Reagen, J. M. Hernández-Lobato, R. Adolf, M. Gelbart, P. Whatmough, G.-Y. Wei, and D. Brooks, "A Case for Efficient Accelerator Design Space Exploration via Bayesian Optimization," in *International Symposium on Low Power Electronics and Design (ISLPED)*, Jul. 2017.
- [49] D. J. Rezende, S. Mohamed, and D. Wierstra, "Stochastic Backpropagation and Approximate Inference in Deep Generative Models," in *International Conference on Machine Learning (ICML)*, Jun. 2014.

- [50] O. Ronneberger, P. Fischer, and T. Brox, "U-Net: Convolutional Networks for Biomedical Image Segmentation," in *Medical Image Computing and Computer-Assisted Intervention (MICCAI)*, N. Navab, J. Hornegger, W. M. Wells, and A. F. Frangi, Eds., 2015.
- [51] D. E. Rumelhart, G. E. Hinton, and R. J. Williams, "Learning Internal Representations by Error Propagation," in *Explorations in the Microstructure of Cognition*, Jan. 1986.
- [52] C. Sakhuja, Z. Shi, and C. Lin, "Leveraging Domain Information for the Efficient Automated Design of Deep Learning Accelerators," in *High-Performance Computer Architecture (HPCA)*, Feb. 2023.
- [53] A. Samajdar, J. M. Joseph, and T. Krishna, "AIrchitect: Automating Hardware Architecture and Mapping Optimization," in *Design, Automation & Test in Europe Conference & Exhibition (DATE)*, Apr. 2023.
- [54] A. Samajdar, J. M. Joseph, Y. Zhu, P. Whatmough, M. Mattina, and T. Krishna, "A Systematic Methodology for Characterizing Scalability of DNN Accelerators using SCALE-Sim," in *International Symposium on Performance Analysis of Systems and Software (ISPASS)*, Aug. 2020.
- [55] L. Sekanina, "Neural Architecture Search and Hardware Accelerator Co-Search: A Survey," *IEEE Access*, 2021.
- [56] K. Seshadri, B. Akin, J. Laudon, R. Narayanaswami, and A. Yazdanbakhsh, "An Evaluation of Edge TPU Accelerators for Convolutional Neural Networks," in *International Symposium on Workload Characterization (IISWC)*, Nov. 2022.
- [57] Y. S. Shao, J. Clemons, R. Venkatesan, B. Zimmer, M. Fojtik, N. Jiang, B. Keller, A. Klinefelter, N. Pinckney, P. Raina, S. G. Tell, Y. Zhang, W. J. Dally, J. Emer, C. T. Gray, B. Khailany, and S. W. Keckler, "Simba: Scaling Deep-Learning Inference with Multi-Chip-Module-Based Architecture," in *Microarchitecture (MICRO)*, Oct. 2019.
- [58] T. Sipola, J. Alatalo, T. Kokkonen, and M. Rantonen, "Artificial Intelligence in the IoT Era: A Review of Edge AI Hardware and Software," in *Conference of Open Innovations Association (FRUCT)*, Apr. 2022.
- [59] I. M. Sobol', "On the Distribution of Points in a Cube and the Approximate Evaluation of Integrals," *Zhurnal Vychislitel'noi Matematiki i Matematicheskoi Fiziki*, no. 4, 1967.
- [60] N. Srinivas, A. Krause, S. Kakade, and M. Seeger, "Gaussian Process Optimization in the Bandit Setting: No Regret and Experimental Design," in *International Conference on Machine Learning (ICML)*, Jun. 2010.
- [61] E.-G. Talbi, "Automated Design of Deep Neural Networks: A Survey and Unified Taxonomy," *Computing Surveys*, no. 2, Mar. 2021.
- [62] J. Vasiljevic, L. Bajic, D. Capalija, S. Sokorac, D. Ignjatovic, L. Bajic, M. Trajkovic, I. Hamer, I. Matosevic, A. Cejkov, U. Aydonat, T. Zhou, S. Z. Gilani, A. Paiva, J. Chu, D. Maksimovic, S. A. Chin, Z. Moudallal, A. Rakhmati, S. Nijjar, A. Bhullar, B. Drazic, C. Lee, J. Sun, K.-M. Kwong, J. Connolly, M. Dooley, H. Farooq, J. Y. T. Chen, M. Walker, K. Dabiri, K. Mabee, R. S. Lal, N. Rajatheva, R. Retnamma, S. Karodi, D. Rosen, E. Munoz, A. Lewycky, A. Knezevic, R. Kim, A. Rui, A. Drouillard, and D. Thompson, "Compute Substrate for Software 2.0," *IEEE Micro*, no. 2, Mar. 2021.
- [63] R. Venkatesan, Y. S. Shao, M. Wang, J. Clemons, S. Dai, M. Fojtik, B. Keller, A. Klinefelter, N. Pinckney, P. Raina, Y. Zhang, B. Zimmer, W. J. Dally, J. Emer, S. W. Keckler, and B. Khailany, "MAGNet: A Modular Accelerator Generator for Neural Networks," in *International Conference on Computer-Aided Design (ICCAD)*, Nov. 2019.
- [64] A. G. Wilson, Z. Hu, R. Salakhutdinov, and E. P. Xing, "Deep Kernel Learning," in *Artificial Intelligence and Statistics (AISTATS)*, May 2016.
- [65] M. Wistuba and J. Grabocka, "Few-Shot Bayesian Optimization with Deep Kernel Surrogates," in *International Conference on Learning Representations (ICLR)*, Oct. 2020.
- [66] S. L. Xi, Y. Yao, K. Bhardwaj, P. Whatmough, G.-Y. Wei, and D. Brooks, "SMAUG: End-to-End Full-Stack Simulation Infrastructure for Deep Learning Workloads," *Transactions on Architecture and Code Optimization (TACO)*, no. 4, Nov. 2020.
- [67] Q. Xiao, S. Zheng, B. Wu, P. Xu, X. Qian, and Y. Liang, "HASCO: Towards Agile Hardware and Software CO-design for Tensor Computation," in *International Symposium on Computer Architecture (ISCA)*, Jun. 2021.
- [68] X. Yang, M. Gao, Q. Liu, J. Setter, J. Pu, A. Nayak, S. Bell, K. Cao, H. Ha, P. Raina, C. Kozyrakis, and M. Horowitz, "Interstellar: Using Halide's Scheduling Language to Analyze DNN Accelerators," in *Architectural Support for Programming Languages and Operating Systems (ASPLOS)*, Mar. 2020.
- [69] A. Yazdanbakhsh, C. Angermueller, B. Akin, Y. Zhou, A. Jones, M. Hashemi, K. Swersky, S. Chatterjee, R. Narayanaswami, and J. Laudon, "Apollo: Transferable Architecture Exploration," *Workshop on ML for Systems*, 2020.
- [70] D. Zhang, S. Huda, E. Songhori, K. Prabhu, Q. Le, A. Goldie, and A. Mirhoseini, "A Full-Stack Search Technique for Domain Optimized Deep Learning Accelerators," in *Architectural Support for Programming Languages and Operating Systems (ASPLOS)*, Feb. 2022.
- [71] F. Zhuang, Z. Qi, K. Duan, D. Xi, Y. Zhu, H. Zhu, H. Xiong, and Q. He, "A Comprehensive Survey on Transfer Learning," *IEEE*, no. 1, Jan. 2021.